JMEPEG (2005) 14:591-595
DOI: 10.1361/105994905X64495

1059-9495/$19.00

Influence of Carburization Followed by Shot Peening on Fatigue Property of 20CrMnTi Steel

Yu-kui Gao, Mei Yao, Qing-xiang Yang, Yan-hui Zhao, Feng Lu, and Xue-ren Wu

(Submitted October 23, 2004; in revised form April 4, 2005)

In this study, the influences of carburization (followed by quenching and low-temperature tempering) followed by shot peening on "apparent" fatigue limits of 20CrMnTi steel specimens were studied and quantitatively analyzed according to the microstructure changes, induced residual stress fields, and position of fatigue crack sources, as well as a micro-meso-process theory for fatigue crack initiation previously proposed by the authors (Ref 6-8). The experimental results show that, although the hardness of the surface layer of carburized specimens is much higher than that of the pseudo-carburized specimens, the improvement effect of carburization on the apparent fatigue limits of specimens is uncertain. It should be related to the possible formation of nonmartensitic microstructure in the surface layer of carburized specimen. After the shot peening, the fatigue limit of specimens was improved and rose to a level about 40% higher than that of the pseudo-carburized specimens. Scanning electron microscopy fractographic analyses show that the fatigue sources, which indicate the weakest link of specimens, in pseudo-carburized and as-carburized specimens are all located at the surface, while after shot-peening, they appear in the interior beneath the hardened layer.

Keywords carburization, fatigue, residual stress, shot peening

1. Introduction

Most automobile gears undergo carburization (followed by quenching and low-temperature tempering) to improve the wear resistance of gear teeth surfaces; however, there are divergent opinions about the influence of carburization on the fatigue strength of gear teeth root (Ref 1). Shot peening is an effective technology for improvement of fatigue strength of most metallic parts, but about its effectiveness for surface heat-treated parts, there are also divergent opinions (Ref 2). The main purposes of this study were to clarify these two problems and to analysis them quantitatively.

2. Materials, Experiments, and Results

Three-point bending fatigue test specimens with dimensions of 10 × 15 × 60 mm were made of a low-carbon steel 20CrMnTi (Fe-0.18C-0.01S-0.03P-1.06Mn-0.27Si-1.26Cr-0.079Ti, wt.%), widely used in China as a gear material. Five types of specimens (Table 1) were used in this work. Carburization was carried out in a furnace in which the carbon potential of atmosphere could be controlled. After carburization, all specimens were directly quenched and then tempered at 180 °C for 2 h. Specimens of type I were copperized before carburization; therefore they were actually "pseudo-carburized" because copperizing can prevent carburizing during heating. Such specimens were used to obtain the information about the material in the interior beneath the hardened layer after carburization. The mechanical properties of 20CrMnTi steel after "pseudo-carburization" are listed in Table 2.

Microstructure analyses and microhardness tests were carried out for the carburized specimens. Some important results are given in Fig. 1 and Table 3. The microstructure of specimen type I, as well as that of the interior of specimen types II and III, was low carbon martensite with nearly the same hardness HV 430. The microstructures of surface layer of specimen types II and III mainly consisted of high-carbon martensite with high hardness near HV 700 at the surface. However, careful observation (Fig. 1f) shows that, on both types of carburized specimen, a thin surface layer exists with nonmartensite microstructure, the depths of which are 30 μm for specimen type II and 10 μm for specimen type III.

Parts of carburized specimens were properly shot peened with an arc height of 0.45 mm (Almen strip type A) and coverage rate of 120% on a pneumatic machine.

The residual stress fields in the surface layer of surface-hardened specimens were determined by an x-ray diffraction method with Cr K_α radiation and a step-by-step electropolishing method (Ref 4). The residual stress distribution curves are illustrated in Fig. 2. It can be seen, after carburization, that the compressive residual stress field was induced in the surface carburized layer with the depth nearly equal to that of carburized layer, but the value is not high (the "valley" value is about 350 MPa). After shot peening, additional residual stress was induced in the layer of about 0.3 mm, and the "valley" value rises to about 900 MPa.

Three-point bending tests were carried out on a high-frequency fatigue test machine with a stress ratio of 0.05. The "apparent" fatigue limit σ_{WA} for 5×10^6 cycles of all types of specimens was determined according to an up-and-down method (Ref 3). The word "apparent" is mainly used for the

Yu-kui Gao, Feng Lu, and **Xue-ren Wu,** Institute of Aeronautical Materials, Beijing 100095, People's Republic of China; and **Mei Yao, Qing-xiang Yang,** and **Yan-hui Zhao,** Key Laboratory of Metastable Materials Science and Technology, College of Materials Science and Engineering, Yanshan University, Qinhuangdao 066004, People's Republic of China. Contact e-mail: yukui.gao@biam.ac.cn.

Table 1 Types of specimens used in this work

Type	Pre-treatment	Carburization	Afterward treatment
I	Copperizing	Same as specimens type II	De-copperizing
II	None	Carburization at 940 °C for 4 h in atmosphere with carbon potential $C_P = 1.0\%$	None
III	None	Carburization at 940 °C for 4 h in atmosphere with carbon potential $C_P = 1.2\%$	None
IV	None	Same as specimens type II	Shot peening
V	None	Same as specimens type III	Shot peening

Table 2 Mechanical properties of pseudo-carburized specimen (specimen type I)

Hardness HV	YS (0.2% offset), MPa	TS, MPa	Elongation, %	RA, %
425	1045	1305	12	45

surface-hardened specimens because in these cases, the determined σ_{WA} is a comprehensive reflection of the properties of the matrix metal and the effect of surface hardening technologies.

Fracture surfaces of broken specimens, tested under the stress level equal or a little higher than the σ_{WA} and with a fatigue life longer than 5×10^5 cycles, were analyzed by scanning electron microscopy (SEM), and the distance of fatigue sources from the surface Z_S was determined. Such a fatigue source should be considered the weakest link of specimens during fatigue. Some typical fractographs are shown in Fig. 3.

3. Analysis and Discussion

3.1 General Considerations

According to the experimental results, three important points should be noted.

- The effect of carburization on the σ_{WA} is quite uncertain. The σ_{WA} of carburized specimen type II is nearly the same in comparison as that of the pseudo-carburized specimen, while that of the carburized specimens type III is improved by about 26%.
- The shot peening improves the σ_{WA} for both types of carburized specimens. The discrepancy of the values of σ_{WA} between two types of carburized specimens is balanced by shot peening and the values of apparent fatigue limit after shot peening, become almost the same (1050 and1070 MPa) for specimens carburized under different conditions.
- The fatigue crack sources in pseudo-carburized, as well as carburized specimens, are all located at the surface, while the fatigue crack sources in shot-peened specimens are located in the interior beneath the shot-peening-effected surface layer with the depth a little larger than that of the compressive residual stress field.

3.2 Calculation of Local Critical Stress for Fatigue Source Formation (Local Fatigue Limit)

The σ_{WA} of pseudo-carburized specimens is the surface fatigue limit σ_{Ws} of the material. Here, the nomenclature "surface fatigue limit" is used to emphasize that the fatigue source in this case is located at the surface. The microstructure of the material in the interior of the carburized specimens is similar to that of the material of the pseudo-carburized specimen; the determined σ_{WA} should be considered also as the σ_{Ws} of the material. However, for surface hardened specimens, in which the residual stress has been induced in their surface layer, the σ_{WA} is not the actual local fatigue limit of the material σ_{WL} at the position of the fatigue crack source. In these cases, σ_{WL} should be calculated according to an equation:

$$\sigma_{WL} = \sigma_{WP} + \sigma_{RS} \quad \text{(Eq 1)}$$

where σ_{WP} is the local applied stress at the position of the fatigue source under the apparent fatigue limit and σ_{RS} is the value of local residual stress. σ_{RS} in the near-surface layer can be determined by the x-ray diffraction method, but, in shot peened specimens, in which the fatigue crack source is located in the deep interior, σ_{RS} can not be determined directly (Ref 5). In these cases, the σ_{RS} values were calculated according to a procedure proposed in Ref 5. The determined or calculated σ_{RS}, as well as the calculated σ_{WL}, are also listed in Table 4.

3.3 Effect of Carburization on Fatigue Limit

As mentioned above, the effect of carburization on the apparent fatigue limit σ_{WA} is quite uncertain. As for the actual local fatigue limit σ_{WL}, the situation is almost the same. It should be noticed that the hardness values of the material at the surface of carburized specimens are higher than that of the pseudo-carburized specimen by about 60%. It is believed that this discrepancy should be related to the nonmartensitic microstructures presenting in the surface layer, which may not reflect in the value of hardness but may destroy the surface structure and decrease the actual fatigue limit. Then the effect of the carburization on the σ_{WA}, as well as the σ_{WL} of the carburized specimen, should be dependent on the carburization technology. As a matter of fact, for carburized specimen type II, in which the depth of the layer with nonmartensitic structure may reach 30 μm, the σ_{WA} is only 740 MPa, even a little lower than that of the pseudo-carburized specimen. For specimen type III, in which the depth of surface layer with nonmartensitic structure is smaller (10 μm), the σ_{WA} reaches 960 MPa. It is believed that if the carburization technology can be controlled more carefully to eliminate the formation of nonmartensitic structure, the σ_{WA} may be increased more significantly.

3.4 Effect of Shot Peening on Fatigue Limit

After shot peening, the σ_{WA} values of both types of carburized specimen are improved and reach about the same level, 1050 MPa, which is about 140% of the fatigue limit of the pseudo-carburized specimen. It should be emphasized that for the shot-peened specimens in this study, the detected fatigue crack sources, which indicate the weakest link of the specimens, are located neither at the surface nor within the compressive residual stress layer but in the internal region beneath

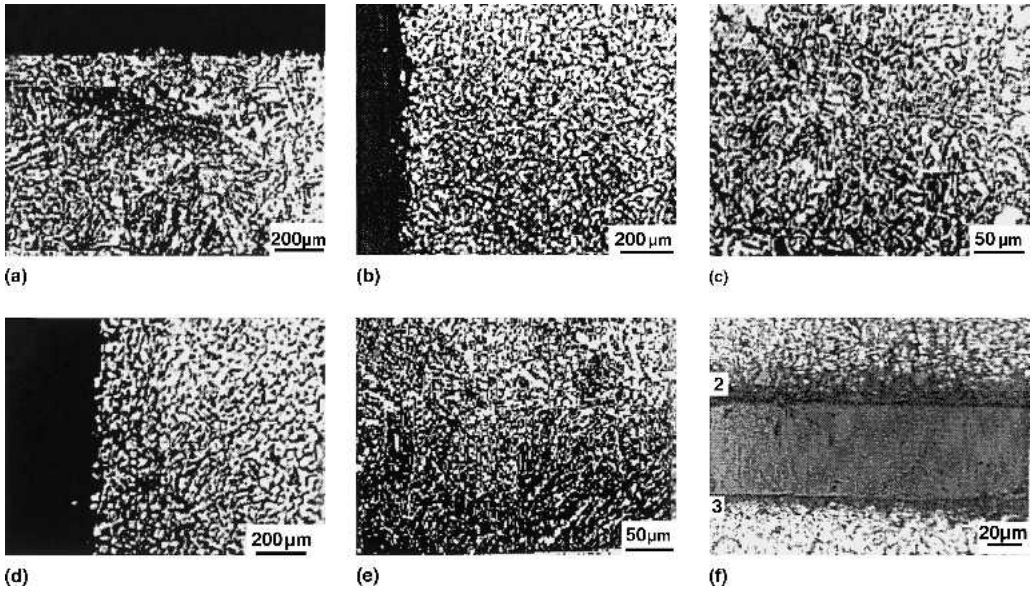

Fig. 1 Microstructures of specimens: (a) specimen type I, (b) surface layer of specimen type II, (c) center of specimen type II, (d) surface layer of specimen type III, (e) center of specimen type III, and (f) comparison of surface layer microstructure of specimens type II and III

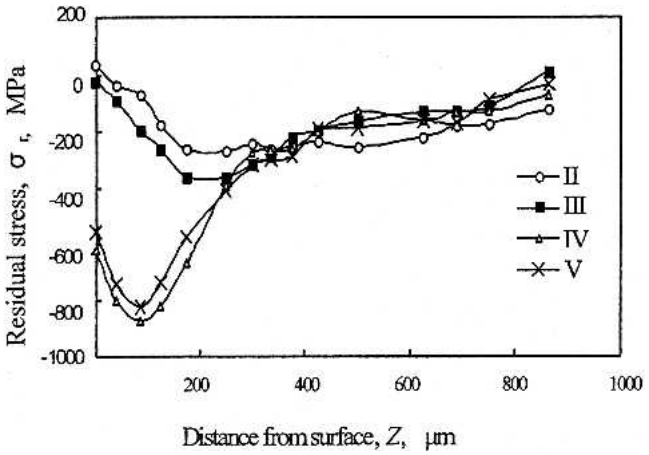

Fig. 2 Residual stress fields of surface-hardened specimens

Table 3 Microhardness test results of carburized specimens

Specimen type	Microhardness, HV		Depth of carburized layer(a), mm
	At the surface	In the center	
I	425	425	
II	660	430	0.95
III	700	425	0.98

(a) From the surface to the point where the micro-hardness gets to that in the center

the carburized layer, where the material is the same as that in the pseudo-carburized specimen. Furthermore, the tensile residual stress was induced during carburization and shot peening; therefore, the improvement of the apparent fatigue limit of specimen should not be directly related to the beneficial effects caused by induction of compressive residual stress or the hardening of the material. The geometric effect, which decreases the applied stress at the position of the fatigue source by only about 3% less than that at the surface, should also not be the main reason for fatigue limit improvement. Therefore, the improvement of the σ_{WA} after shot peening must be related to the hardening of the surface to definite degree and the transfer of the weakest link from the surface to the interior. The σ_{WL} at the fatigue source in these two cases is nearly the same, about 1030 MPa (Table 4), which is higher than the surface fatigue limit σ_{Ws} of the material in pseudo-carburized specimens, or that in the interior of carburized specimens, by about 36%. Such σ_{WL} is actually the internal fatigue limit σ_{Wi} of the material in the interior because the weakest link is located beneath the hardened layer for both types of the carburized specimen.

The above-mentioned results can be analyzed quantitatively according to a micromeso-process theory of fatigue source evolution, which we have proposed elsewhere (Ref 6-8). The fundamental considerations of this theory are as follows: The evolution of fatigue source consists of two main steps, the initiation of fatigue cracks in one or several weak grains and the propagation of one of the initial cracks into its neighboring grains. In polycrystalline material, all processes related with these two steps will start in the range of individual weak grains, but they must be restricted by their neighboring grains. That is to say, such processes within individual grains (called "micro-processes") cannot occur and develop without the harmonious processes occurring within their neighboring grains (called as "meso-processes"). Besides that, it should be emphasized that all related processes have stochastic characters. According to these considerations, in order for the evolution of fatigue source to take place, not only the mechanical condition, but also the probabilistic and harmonizing demands should be satisfied, and it can be concluded that the dominant process for fatigue source evolution is the formation of so-called "cyclic meso-yielding areas" (CMYAs) surrounded by elastically deformed mass, and the (apparent) fatigue limit for a given number of stress cycles of a metal/metallic specimen is actually

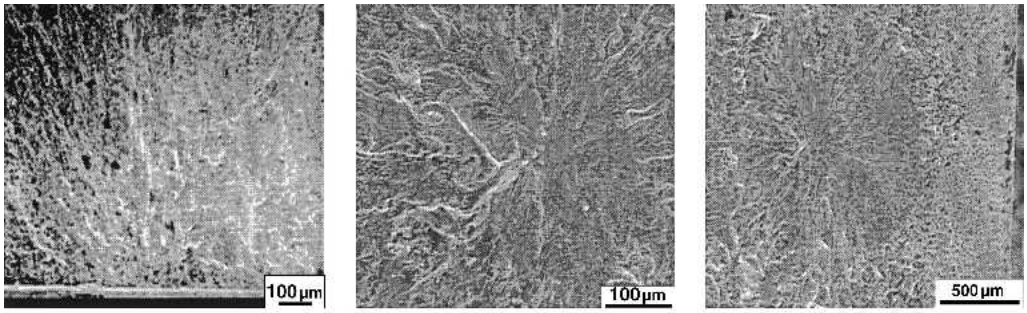

Fig. 3 Fractographs of fatigue fracture surfaces: (a) specimen type I, (b) specimen type IV, and (c) specimen type V

Table 4 Fatigue test results of 20CrMnTi steel

Type of specimen	Apparent fatigue limit, σ_{WA}, MPa	Distance of fatigue source from surface, Z_S, mm	Residual stress at position of fatigue source σ_{RS} (a), MPa	Local fatigue limit, σ_{WL}, MPa
I	760	0 (at the surface)	0	760
II	740	0	+32	772
III	960	0	−20	940
IV	1050	1.23	+185	1025
V	1070	1.33	+190	1030

(a) (+) tensile, (−) compression

the stress to form CMYAs with a critical size, which nearly cannot supply the needed probabilistic and harmonious demands for fatigue source formation in the service period. Such stress for fatigue crack source formation (fatigue limit) is very different when the fatigue source is at the surface or in the interior. The dislocation motion in individual weak grains near the surface is only restricted by their neighboring grains from inner side and is free from its surface side, while that in grains in the interior is restricted by all-surrounding grains. Then, the stress as well as its critical value (the local fatigue limit) for CMYA formation at the surface should be lower than that in the interior. This is the reason the fatigue source evolution nearly always occurs at the surface and the fatigue limit of metal is always lower than its yield strength for surface-unhardened specimens. However, when the metallic parts are surface hardened, the material at the surface becomes stronger; then the cyclic meso-yielding may occur in comparatively weaker interior under the hardened layer. In this case, the stress for formation of critical CMYAs in the interior should be considered. This is to say, there should be two fatigue limits for the same metal: the surface fatigue limit σ_{Ws}, which is the fatigue limit of metal in common sense, and the internal fatigue limit σ_{Wi}, which is higher than σ_{Ws} and is active for surface-hardened specimens. It can be deduced that the ratio of σ_{Wi}/σ_{Ws} is a value lower but close to $\sqrt{2}$. Experimental results obtained on about twenty metals show the ratios of σ_{Wi}/σ_{Ws} all lie in the range of 1.35-1.40, coincident with the theoretically predicted value.

The results in this work also can be analyzed by the above-mentioned considerations. The σ_{WL} of specimen types IV and V listed in Table 4 are actually the σ_{Wi} of the pseudo-carburized material, which is 1.36 times the σ_{Ws} of the same material. This value coincides with the theoretically predicted one quite well. Because the σ_{Wi} is higher than σ_{Ws}, although the fatigue sources of these specimens are located in the unhardened interior, their σ_{WA} is still improved. Obviously, the σ_{WA} of specimen with internal fatigue source σ_{WAi} (expressed in nominal stress at the surface) can be determined by:

$$\sigma_{WAi} = k(\sigma_{Wi} - \sigma_{RS}) \quad \text{(Eq 2)}$$

where σ_{Wi} is the internal fatigue limit, σ_{RS} is the (tensile) residual stress at the position of fatigue source and k is a factor considering the difference of the applied stress at the surface and that at the position of fatigue source.

4. Conclusions

The effect of carburization on the three-point bending (apparent) fatigue limit of the 20CrMnTi steel specimen is quite uncertain. In this study, the apparent fatigue limit of the carburized specimen may change from 98 to 126% of the pseudo-carburized specimen. This discrepancy should be related to the different surface layers with nonmartensite structure formed during carburization.

Shot peening improves the apparent fatigue limits of both types of the carburized specimen. The values of apparent fatigue limit after shot peening become almost the same for specimens carburized under different conditions and gets to about 1060 MPa, 40% higher than that of the pseudo-carburized specimen.

The fatigue crack sources in pseudo-carburized and carburized specimens are all located at the surface while the fatigue crack sources in shot-peened specimens are located in the interior, beneath the shot-peening-effected surface layer with the depth a little larger than that of the compressive residual stress field, where the material has not been hardened, and the tensile residual stress has been induced. The improvement of apparent fatigue limit in these cases is due to the fact that the internal fatigue limit of metal is higher than its surface fatigue limit by about 36%.

References

1. Y. Gao, "Quantitative Study on Influence of Chemical Heat Treatment on Apparent Fatigue Limit of Structural Steel Specimens," Master's Thesis, Yanshan University, Qinhuangdao, 2000 (in Chinese)
2. Y. Gao and M. Yao, Quantitative Study on Influence of Chemical Heat Treatment on Apparent Fatigue Limit of 40Cr Steel, *J. Aeronautical Mater.,* Vol 22 (No. 4), 2002, p 21-25 (in Chinese)
3. G.E. Dieter, *Mechanical Metallurgy,* 2nd ed., McGraw-Hill, Inc., 1976, p 411-412
4. D. Zhang and J. He, *Residual Stress Analysis by X-ray Diffraction and Its Function,* Xi'an Jiaotong University Press, Xi'an, People's Republic of China, 1999, p 66-73 (in Chinese)
5. J. Li and M. Yao, Tensile Residual Stress Field Induced by Shot Peening and Internal Fatigue Limit of Materials. *Acta Aeronaut. Astronaut. Sin.,* Vol 11A, 1990, p 511-519 (in Chinese)
6. Y. Gao, M. Yao, and J. Li, An Analysis of Residual Stress Fields Caused by Shot Peening. *Metall. Mater. Trans. A.,* Vol 33 (No. 6), 2002, p 1775-1778
7. Y-K. Gao, F. Lu, Y-F. Yin, and M. Yao. Effect of Shot Peening on Fatigue Property of 0Cr13Ni8Mo2Al Steel, *Mater. Sci. Technol.,* Vol 19 (No. 3), 2003, p 372-374
8. Y. Gao, M. Yao, P. Shao, and Y. Zhao, Another Mechanism for Fatigue Strength Improvement of Metallic Parts by Shot Peening, *J. Mater. Eng. Perf.,* Vol 12 (No. 5), 2003, p 507-511